Title

Atrophin 2 recruits histone deacetylase and is required for the function of multiple signaling centers during mouse embryogenesis

Journal

Development, 131(1)

ISSN

0950-1991

Authors

Zoltewicz, J S
Stewart, N J
Leung, R
et al.

Publication Date

2004

Peer reviewed

Atrophin 2 recruits histone deacetylase and is required for the function of multiple signaling centers during mouse embryogenesis

J. Susie Zoltewicz, Nicola J. Stewart, Ricky Leung and Andrew S. Peterson*

Department of Neurology and the Ernest Gallo Clinic and Research Center, University of California at San Francisco, 5858 Horton Street, Emeryville, CA 94608, USA
*Author for correspondence (e-mail: andpete@itsa.ucsf.edu)

Accepted 30 September 2003

Development 131, 3-14
Published by The Company of Biologists 2004
doi:10.1242/dev.00908

Summary

Atrophins are evolutionarily conserved proteins that are thought to act as transcriptional co-repressors. Mammalian genomes contain two atrophin genes. Dominant polyglutamine-expanded alleles of atrophin 1 have been identified as the cause of dentatorubral-pallidoluysian atrophy, an adult-onset human neurodegenerative disease with similarity to Huntington's. In a screen for recessive mutations that disrupt patterning of the early mouse embryo, we identified a line named openmind carrying a mutation in atrophin 2. openmind homozygous embryos exhibit a variety of patterning defects that first appear at E8.0. Defects include a specific failure in ventralization of the anterior neural plate, loss of heart looping and irregular partitioning of somites. In mutant embryos, Shh expression fails to initiate along the anterior midline at E8.0, and Fgf8 is delocalized from the anterior neural ridge at E8.5, revealing a crucial role for atrophin 2 in the formation and function of these two signaling centers. Atrophin 2 is also required for normal organization of the apical ectodermal ridge, a signaling center that directs limb pattern. Elevated expression of atrophin 2 in neurons suggests it may interact with atrophin 1 in neuronal development or function. We further show that atrophin 2 associates with histone deacetylase 1 in mouse embryos, providing a biochemical link between Atr2 and a chromatin-modifying enzyme. Based on our results, and on those of others, we propose that atrophin proteins act as transcriptional co-repressors during embryonic development.

Key words: Atrophin, Forebrain, Co-repressor, Mouse, Notochord, ANR

Introduction

The vertebrate neural plate is induced and patterned through the concerted action of a series of signaling centers (Beddington and Robertson, 1998; Gerhart, 2001; Harland and Gerhart, 1997; Rubenstein and Beachy, 1998; Rubenstein et al., 1998). In mouse embryos prior to gastrulation, neural development in the epiblast is initiated by signals emanating from the anterior visceral endoderm (AVE). During gastrulation, neural pattern is further defined by signals produced by the anterior end of the primitive streak, the node (Beddington and Robertson, 1999). The node, functionally similar to the amphibian Spemann Organizer, gives rise to definitive endoderm, as well as to the prechordal plate (pcp) and notochord. (Beddington and Robertson, 1999; Kinder et al., 2001; Spemann and Mangold, 1924). Pcp and presumptive notochord cells populate the ventralmost embryonic midline during day 8 of development (E8.0). These midline cells produce signals that pattern the developing neural tube along its anteroposterior and dorsoventral axes (Camus et al., 2000; Hemmati-Brivanlou et al., 1990; Kazanskaya et al., 2000; Martinez-Barbera and Beddington, 2001; Mukhopadhyay et al., 2001; Saude et al., 2000; Shawlot et al., 1999; Zoltewicz and Gerhart, 1997). One ventralizing signal produced by both the pcp and the notochord is sonic hedgehog (Shh) (Echelard et al., 1993; Epstein et al., 1999). Embryos lacking Shh exhibit ventral midline defects along the length of the neuraxis, from cyclopia to loss of notochord and floorplate (Chiang et al., 1996), demonstrating that both brain and spinal cord require this signal to develop normally (Briscoe et al., 1999; Ericson et al., 1995; Gunhaga et al., 2000; Shimamura and Rubenstein, 1997).

The anterior neural ridge (ANR), located at the rostral margin of the neural plate, is a signaling center required for forebrain development, specifically for elaboration of pattern in the most anterior subregion of the brain, the telencephalon (Eagleson and Dempewolf, 2002; Shimamura and Rubenstein, 1997). One of the signals secreted by the ANR beginning at E8.0 is Fgf8 (Crossley and Martin, 1995). Mutants with reduced *Fgf8* expression in the ANR and its derivatives, such as *Hex*$^{-/-}$, *Hesx1*$^{-/-}$ and *oto*$^{-/-}$ embryos, exhibit incomplete telencephalic development (Martinez-Barbera and Beddington, 2001; Martinez-Barbera et al., 2000; Zoltewicz et al., 1999). In addition, mouse embryos expressing Fgf8 from a hypomorphic allele develop reduced telencephalic structures (Meyers et al., 1998). These studies together define a prominent role for Fgf8 in ANR function.

The study of mutant alleles is a powerful approach for understanding gene function. We have carried out a random chemical mutagenesis screen in mice, aimed at identifying recessive mutations affecting early embryonic patterning (Hentges et al., 1999). In this screen, we uncovered an embryonic lethal mutation in an atrophin family member. We

have named the mutant allele *openmind* (*om*), and the gene *atrophin-2* (*Atr2*). Atr2, known in human as Arginine (R) Glutamic Acid (E) Repeat Encoding or RERE, was first described as an atrophin 1 (Atr1)-related protein that could heterodimerize with Atr1 (Waerner et al., 2001; Yanagisawa et al., 2000). Atr1 (Drpla – Mouse Genome Informatics) has been well studied because it causes a human neurodegenerative disease known as dentatorubral-pallidoluysian atrophy (DRPLA) when its polyglutatmine tract is abnormally expanded. Atr2 is distinguished from Atr1 in that it does not have a polyglutamine tract, but it does bind tightly to glutamine-expanded Atr1 (Yanagisawa et al., 2000), suggesting that Atr2 has a role in DRPLA disease development or progression. DRPLA is one of a family of nine polyglutamine diseases that includes Huntington's disease, Spinal and Bulbar Muscular Atrophy, and several spinocerebellar ataxias. Although the proteins encoding polyglutamine tracts are distinct in each disease, there is evidence for a similar underlying pathogenic mechanism involving disruption of gene regulation in the nucleus (McCampbell et al., 2001; Nucifora et al., 2001; Ross, 2002). The normal function of vertebrate Atr1 is not understood but, as it binds to Eto1, a component of nuclear co-repressor complexes, a role in transcriptional repression has been proposed (Wood et al., 2000).

Whereas mouse and human genomes contain two distinct atrophin genes, the *Drosophila* genome contains only one, known as *Atro* or *Grunge*. Mutation of this gene causes a variety of defects, including disruption of embryonic patterning (Erkner et al., 2002; Fanto et al., 2003; Zhang et al., 2002). Atro binds to the Even skipped (Eve) and Huckebein transcription factors, and acts as a co-repressor for Eve (Zhang et al., 2002). The *C. elegans* genome also has a single atrophin ortholog, *egl-27*, which is also required for the development of embryonic pattern (Ch'ng and Kenyon, 1999; Herman et al., 1999; Solari et al., 1999). Atr2, Atro and EGL-27, but not Atr1, each has N-terminal homology to metastasis-associated protein 2 (Mta2), a core component of the NuRD (Nucleosome Remodeling and Deacetylase) complex (Zhang et al., 1999). NuRD and other histone deacetylase complexes silence genes by altering chromatin structure such that the DNA becomes inaccessible to transcriptional activators (Ng and Bird, 2000). Because of their homology to Mta2, it has been proposed that the vertebrate, fly and worm atrophins may regulate transcription by acting in conjunction with histone deacetylase complexes (Solari and Ahringer, 2000; Solari et al., 1999; Zhang et al., 2002). However, no biochemical evidence showing association of an atrophin with such a complex has yet been reported.

Here, we report that *Atr2*-mutant embryos exhibit diverse developmental defects, and we focus on the role of Atr2 in patterning the anterior neural tube. We provide evidence that anterior neural defects are caused by disruption of two signaling centers, namely the anterior embryonic midline and the ANR. We show that the N terminus of Atr2 is sufficient to recruit histone deacetylase 1 (Hdac1), but not other NuRD core subunits, suggesting that Atr2 is part of a novel histone deacetylase complex. We propose that the molecular mechanism underlying *om* defects involves loss of function of this complex, and specific disregulation of *Shh* and *Fgf8*.

Materials and methods

Mapping and cloning

Adult BTBR (Jax) males were mutagenized with ENU by intraperitoneal injection (Shedlovsky et al., 1986). Mutagenized males were then backcrossed to C57BL/6J (B6; Jax) mice, and progeny intercrossed to identify *om* carriers. Carriers were then genotyped using polymorphic microsatellite markers from MIT (http://www-genome.wi.mit.edu/) that vary by size between BTBR and B6. After extensive backcrossing, the mutation was localized to an ~2 Mb interval flanked by D4Mit127 and D4Mit190. Candidate genes were picked by examining the human syntenic interval, using the UCSC Human Genome Browser (http://genome.ucsc.edu/). PCR amplification and sequencing of the mouse ortholog of *Atr2* revealed a point mutation within this gene (see Results).

The full-length mouse *Atr2* cDNA was cloned by RT-PCR and sequences verified by comparing with consensus sequences derived from NCBI and celera databases. 3× flag tags were added to the N termini of Atr2 proteins using the 3×Flag-CMV7 expression vector (Sigma). Fragments of Atr2 were created by dividing the cDNA into N-terminal (N-Atr2) and C-terminal (C-Atr2) coding portions using a unique *Eco*RI site between the SANT- and GATA-coding sequences.

Labeling of embryos, histology and 5′ RACE

Embryos of desired ages were obtained by carrying out timed matings between genotyped carriers. Whole-mount in situ hybridization was performed as described (Zoltewicz et al., 1999). The Atr2/β-galactosidase fusion protein in PT026 embryos was visualized with X-gal substrate using standard procedures. Some embryos were embedded in paraplast and sectioned at 7 μm using standard procedures; others were embedded in agarose and vibratome-sliced. 5′ RACE was performed using the First Choice RLM-RACE kit from Ambion.

Co-immunoprecipitation

Flag-tagged Atr2 constructs were transiently transfected into 293 cells using Lipofectamine Plus (Invitrogen). Transfected cells were harvested after 24 hours in culture and lysed in Ripa buffer [150 mM NaCl, 50 mM Tris (pH 7.5), 0.5% sodium deoxycholate, 0.5% NP-40, 0.1% SDS, complete protease inhibitors (Roche)]. Nucleic acids were degraded by benzonase nuclease (Novagen) treatment. An equal volume of buffer, similar to Ripa but lacking denaturing detergents, was added and the insoluble debris pelleted. Soluble extracts were added to M2 anti-flag beads (Sigma) pre-blocked with BSA, and extracts plus beads were nutated for one hour at 4°C. Beads were washed 5 times, then bound were proteins eluted, resolved on 4-12% Bis-Tris gels (Fig. 5B) or 3-8% Tris-Acetate gels (Fig. 5C,D), and transferred to PVDF membrane (Amersham) using the XCell II system (Invitrogen). Blots were probed with anti-flag M5 (Sigma), anti-Hdac1, anti-RbAp46, anti-RbAp48 (Affinity Bioreagents) and anti-Atr1 (Santa Cruz). The 286-1 antibody was created by immunizing rabbits with a peptide matching the C terminus of Atr1 (Synpep). It was affinity purified and DSS-crosslinked (Pierce) to protein G sepharose.

Results

Atr2 has diverse roles in early embryonic development

We identified an *Atr2* mutation in a screen for ENU-induced recessive mutations causing developmental defects in the forebrain (Hentges et al., 1999). Loss of Atr2 causes a failure of the anterior neural tube to close, and a fusion of the telencephalic and optic vesicles by 9.5 days of gestation (E9.5) (Fig. 1B,D). Based on the open neural tube in the forebrain region, we named the mutant *openmind* (*om*). Homozygous *om*

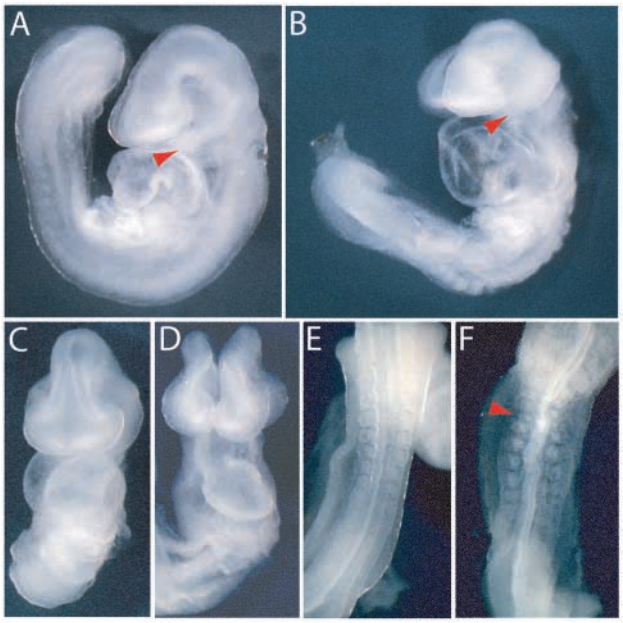

Fig. 1. *openmind* embryos exhibit diverse developmental defects by E9.25. A wild-type embryo at E9.25 (A) and an *om* homozygous littermate (B) of the same stage and size are shown in side views. The mandibular component of the first branchial arch is well developed in the wild type but is poorly developed in the *om* embryo (red arrowheads). The *om* heart is abnormally dilated and is near failure. (C) The anterior neural tube is fully closed by E9.25 in a normal embryo (shown in front view with tail removed), the heart is looped, and the optic vesicles are visible. (D) In the *om* mutant, the anterior neural tube fails to close and is abnormally thickened, the heart remains as an unlooped tube, and the optic vesicles are morphologically absent. (E) Wild-type somites are uniform, and the neural tube is smooth and straight at the midline in this dorsal view of the tail. (F) *om* somites are irregular in size (red arrowhead points to a small somite) and the neural tube is kinked.

mutant embryos have a variety of other defects that indicate diverse roles for Atr2 during development. The first branchial arch is reduced in size, with a deficit in the mesenchymal component (Fig. 1B, arrowhead). The heart tube fails to loop (Fig. 1D). Defects in somitogenesis are revealed by the variable occurrence of irregularly shaped and sized somites (Fig. 1F, arrowhead). Morphological irregularities in mutants first appear at E8.25. Mutants are recovered at Mendelian ratios up to E9.5 but, by E11.5, no mutant embryos are found. All *om* homozygotes die, without exception, as a result of cardiac failure shortly after E9.5. The phenotype is 100% penetrant on the C57Bl6/J×BTBR background, as well as after outcrossing to the wild-type strain *Castaneus Ei*. The expressivity is stable; i.e. there is little variability in the phenotype.

The *om* mutation was mapped to the distal portion of chromosome 4, in a region of synteny with human 1p36. *Atr2* (or *RERE*) was among the genes in the *om* candidate interval (Fig. 2A). RT-PCR of approximately 1200 bases of the N terminus of *Atr2* cDNA from wild-type tissues yielded two products, one major transcript, including all exons, and a minor alternatively spliced form lacking exon 5 (Fig. 2B). In the mutant, these products were each about 70 bases shorter than in wild type. In addition, the mutant transcripts amplified relatively poorly suggesting a decreased expression level. Sequencing of products revealed that the 72-base fourth exon was missing from mutant *Atr2* cDNAs (Fig. 2B). Sequencing of mutant genomic DNA revealed a single base change in the exon 4 splice donor, a T to A transition (Fig. 2C). The only detected messages in *om* embryos showed exon 3 spliced to exon 5 for the main transcript, or exon 3 spliced to exon 6 for the alternative splice, demonstrating that mutation of the GT splice signal to GA prevented inclusion of exon 4. No messages with exon 3 joined to exon 5 or exon 6 were observed in wild-type embryos. Because exon 3 and exons 5/6 have different reading frames, mutant splicing events generate frameshifts in both the full-length and alternatively spliced messages. As a result, these messages are destabilized, and are virtually undetectable by whole-mount in situ hybridization with a 5′ probe (Fig. 2D). Because no in-frame transcripts can be produced, the *om* mutation is likely to produce a null allele.

To obtain additional mutant alleles of *Atr2*, we turned to a library of insertion mutations produced in embryonic stem cells by Dr Skarnes' group (http://baygenomics.ucsf.edu/). Survey of this gene trap database revealed insertions within the 12th intron of the *Atr2* gene (Fig. 2A). Two cell lines carrying independent insertions were selected, called *PT026* and *XE778*, and mice were made. These mice express mutant versions of Atr2, composed of several hundred N-terminal amino acids of Atr2 fused to β-galactosidase (βgal). Heterozygous mice had no apparent phenotype, indicating that the fusion proteins did not have dominant-negative activity. *PT026* heterozygotes were crossed with *om* carriers to test whether the *om* phenotype is indeed caused by mutation of *Atr2*. Compound heterozygous embryos duplicated the *om* phenotype, showing characteristic forebrain, heart, first branchial arch and somite defects (Fig. 2E). Because compound mutants have the same phenotypic abnormalities as *om* homozygotes, we conclude that disruption of the *Atr2* gene is responsible for the *om* phenotype.

PT026 carriers were also intercrossed to produce *PT026* homozygous embryos. These mutants ranged from severely affected (identical to *openmind* homozygotes) to apparently normal, suggesting the *PT026* allele might be hypomorphic. RT-PCR analysis confirmed the existence of the wild-type transcript in *PT026* mutants (not shown), indicating that *PT026* is indeed a hypomorphic allele. Even though some homozygous embryos looked normal at E9.5, no homozygous pups were ever recovered, indicating that the quantity of wild-type message is not sufficient to rescue viability. However, this report is not intended to be a detailed characterization of the *PT026* mutant phenotype. Here, we used *PT026* for two limited purposes: to confirm correct identification of the mutated gene and to define the wild-type expression pattern of Atr2.

A close examination of *Atr2* genomic sequences revealed the existence of a second CpG island in the 12th intron (Fig. 2A). To determine whether this island represented an internal promoter producing another *Atr2* transcript, 5′ Race was performed. This analysis revealed a transcript that initiates within the second CpG island, and it was named *Atr2S* for *Atr2* short form. Seven identical clones representing the 5′ most end of the *Atr2S* mRNA were isolated, revealing that the *Atr2S* transcript contains about 100 bases of unique 5′ GC-rich leader sequence that splice into exon 13 (data not shown). Because *Atr2S* initiates far downstream of the *openmind* point mutation, and because the *om* mutation affects expression of the full-

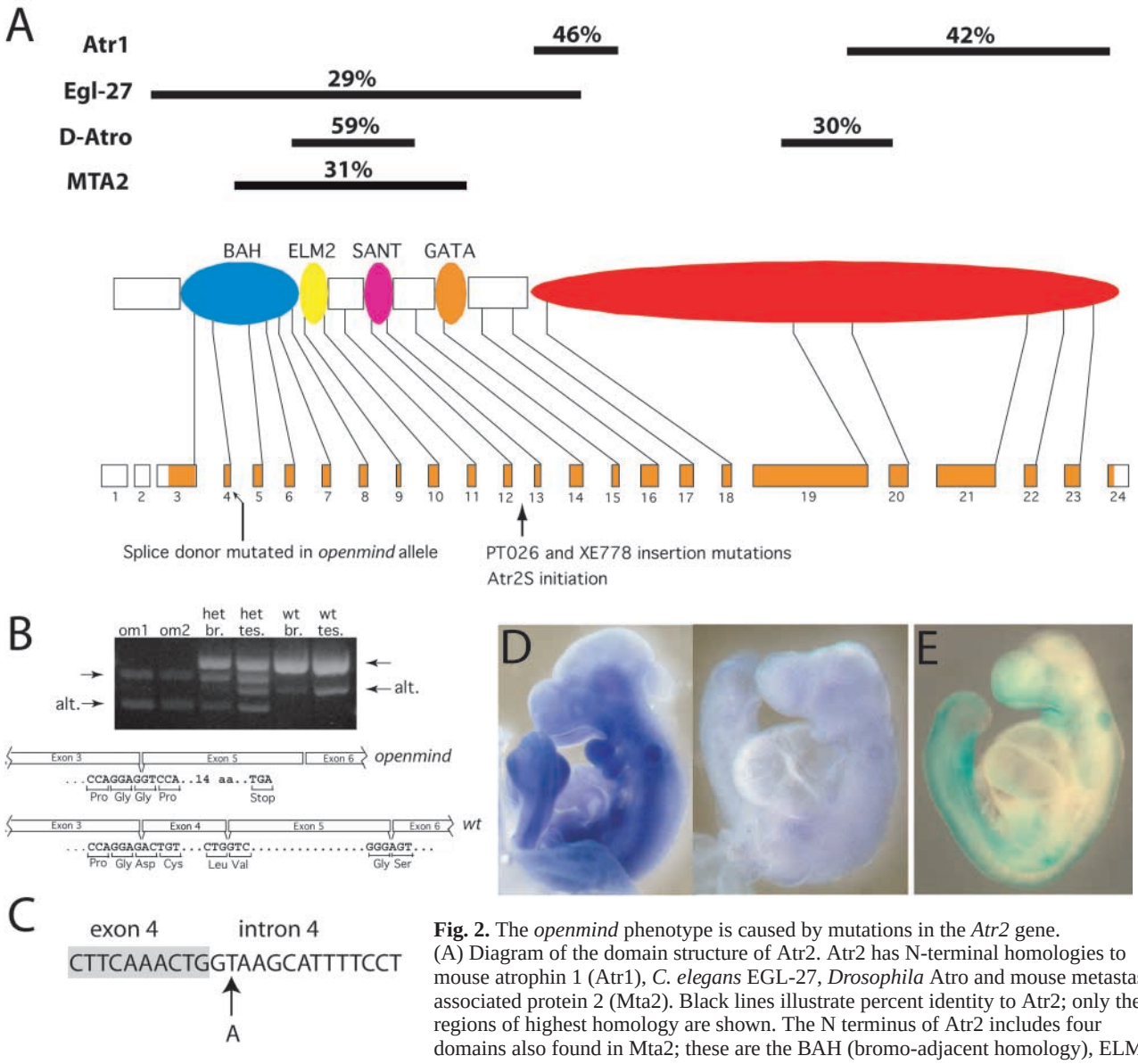

Fig. 2. The *openmind* phenotype is caused by mutations in the *Atr2* gene. (A) Diagram of the domain structure of Atr2. Atr2 has N-terminal homologies to mouse atrophin 1 (Atr1), *C. elegans* EGL-27, *Drosophila* Atro and mouse metastasis associated protein 2 (Mta2). Black lines illustrate percent identity to Atr2; only the regions of highest homology are shown. The N terminus of Atr2 includes four domains also found in Mta2; these are the BAH (bromo-adjacent homology), ELM2 (EGL-27 and Mta1 homology 2), SANT (SWI3, ADA2, N-CoR and TFIIIB) and GATA (zinc finger) domains. The C terminus of Atr2 (red oval) is homologous to Atr1. The exon structure of the *Atr2* gene is shown with respect to the domain structure of the encoded protein. Exons are numbered from the 5′ end of the gene; coding sequences are orange, non-coding sequences white. Positions of the *om* mutation, insertion alleles and the Atr2S initiation site are indicated. (B) RT-PCR of ~1200 bases of the amino end of *Atr2* from *om* mutant embryos, and heterozygous and wild-type tissues. The primers amplify two bands from wild-type brain (br.) and testis (tes.), one full-length (right upper arrow) and the other a minor alternatively spliced form lacking exon 5 (right lower arrow). By contrast, shorter fragments amplify from *om* mutants (left arrows). Brain and testis from heterozygous animals show all transcripts. Mutant and wild-type full length fragments are illustrated. The mutant cDNA has exon 3 spliced to exon 5, whereas wild-type cDNAs always include exon 4. The reading frames of exons 3 and 5 are different, creating a stop codon. (C) The genomic sequence of the 3′ end of exon 4 (shaded) and the start of intron 4 is shown. *om* homozygotes have an ENU-induced single base change of T to A; this mutation destroys the splice donor causing exon 4 to be omitted from the mutant mRNA. (D) Whole-mount in situ hybridization for *Atr2* with a 5′ probe at E9.5 reveals a dramatic reduction in *Atr2* mRNA levels in mutant embryos (right) compared with normal littermates (left). (E) At E9.5, a βgal-stained compound heterozygote with the $Atr2^{om}/Atr2^{PT026}$ genotype clearly duplicates the *om* phenotype (see text).

length *Atr2* only (Fig. 5D), *Atr2S* does not contribute to the *om* phenotype and will be characterized elsewhere.

Atr2 is widely expressed during embryonic development

The expression of Atr2 in the developing embryo was examined using β-galactosidase (βgal) staining to detect the PT026 fusion protein, and whole-mount in situ hybridization to detect the endogenous mRNA. In order to visualize only full-length *Atr2*, a 5′ specific RNA probe having no sequences in common with *Atr2S* was used for the in situ hybridization. The expression patterns visualized by these two methods were

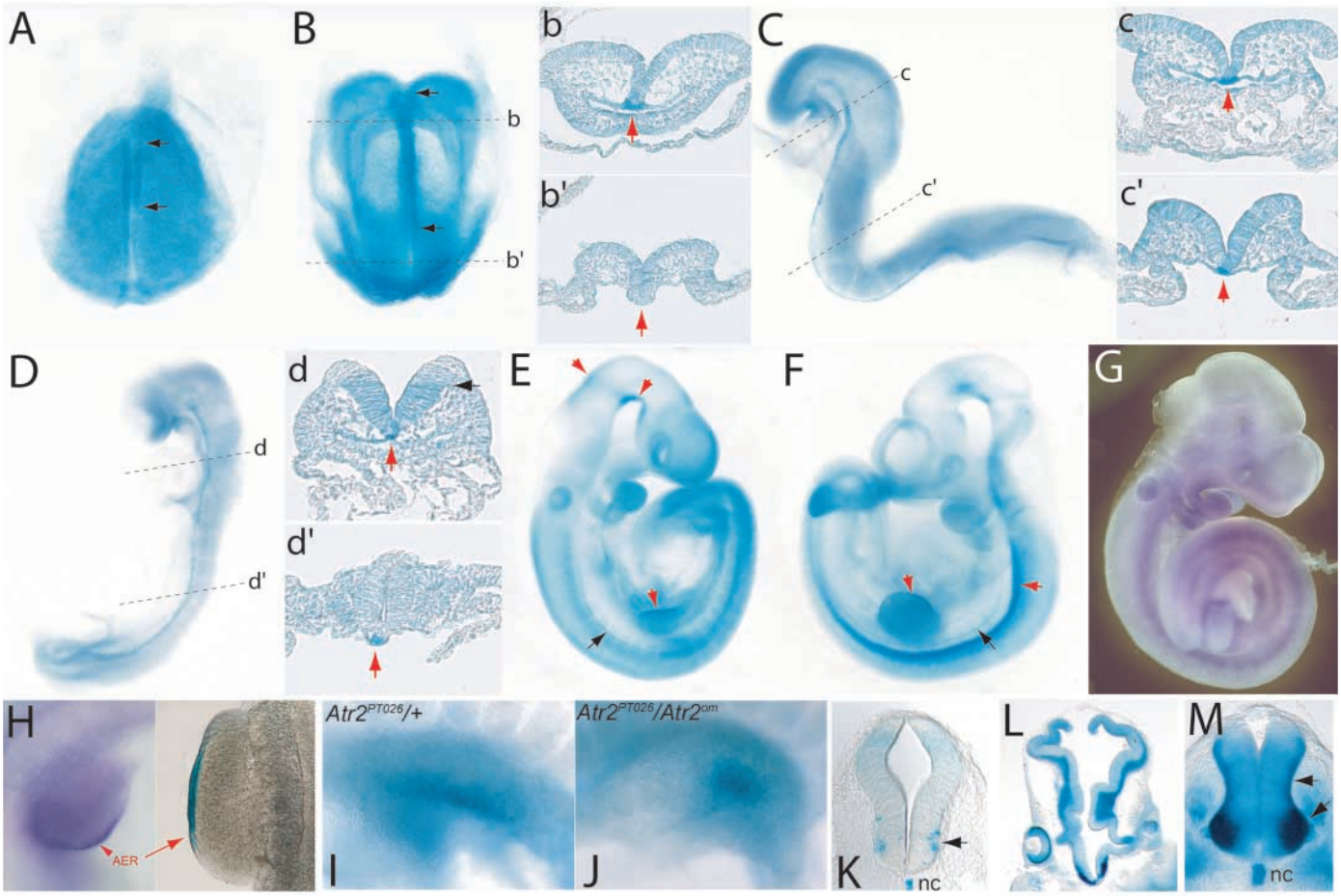

Fig. 3. Atr2 expression is elevated in the developing notochord, apical ectodermal ridge and neurons. A time course of Atr2 expression, from E8.0 through E11.5, is illustrated using the *PT026* Atr2-βgal fusion protein. (A) At E8.0, Atr2 is expressed throughout the embryo and is elevated in the anterior midline (region between arrows; front view, anterior up; this embryo has been flattened). (B) At E8.25, Atr2 shows a more pronounced elevation in the anterior midline (arrows). (b) A transverse section through the anterior of the embryo in B shows elevated expression in midline cells (red arrow). (b′) A more posterior section from the same embryo shows no elevated expression in the posterior midline (red arrow). (C) At E8.5, Atr2 is elevated throughout the anteroposterior extent of the notochord and is downregulated in the heart. (c,c′) Transverse sections confirm elevated expression in anterior and posterior regions of the notochord (red arrows). (D) At E8.75, expression is increased in the ventral brain. (d) A section through the hindbrain reveals continued expression in the notochord (red arrow), and the beginning of elevation in the ventral brain (black arrow). (d′) A more posterior section shows uniform expression in the spinal cord, and upregulation in the notochord (red arrow). (E) At E9.5, additional sites of elevation besides the notochord (black arrow) appear, including the apical ectodermal ridge, the isthmus and the ventral diencephalon (red arrows). (F) At E10.5, sites of elevation include the notochord (black arrow), the AER, and spinal and brain neurons (red arrows). (G) A wild-type embryo at E9.75, showing that the pattern of *Atr2* transcripts detected with a 5′ RNA probe is similar to the fusion protein at E10.5. (H) A wild-type forelimb bud at E9.5 shows concentrated expression of *Atr2* mRNA in the AER (left). A section through the forelimb bud of an E9.5 $Atr2^{PT026}$/+ embryo shows βgal expression in the AER (right). (I) Formation of the AER occurs normally in $Atr2^{PT026}$/+ embryos at E9.0. (J) The AER is defective in $Atr2^{PT026}/Atr2^{om}$ embryos at E9.0. (K) A transverse section through the caudal hindbrain at E9.5 shows elevated expression in ventrolateral neurons (arrow). (L) A horizontal section through the optic region at E11.5 shows expression in telencephalic and diencephalic neurons. (M) A transverse section at sacral level at E11.5 shows high levels of expression in spinal cord neurons.

similar. Atr2 expression was examined in detail from E7.5 through E11.5, using *PT026* heterozygotes. Atr2 expression was observed in every cell of the embryo at all these stages. Some regions, such as the heart and dorsal neural tissues, downregulate expression but do not lose it entirely. Atr2 was expressed uniformly at E7.5 throughout the embryo in all three germ layers (not shown). At early headfold, expression is mostly uniform but begins to be upregulated in the anterior portion of the embryonic midline (Fig. 3A). By E8.25, expression is strongly elevated in the anterior midline, but remains at a uniform level posteriorly (Fig. 3B,b,b′). By E8.5, expression is upregulated along the entire notochord (Fig. 3C,c,c′). At E8.75, expression remains high in the notochord, and begins to elevate ventrally in the anterior CNS (Fig. 3D,d,d′). At E9.5, additional sites of elevated expression appear, including the apical ectodermal ridge, the isthmus, the ventral diencephalon and ventral neurons (Fig. 3E,K). At E10.5, neurons in the spinal cord and brain strongly upregulate expression (Fig. 3F). The mRNA pattern at E9.75 is similar to that of the fusion protein at E10.5 (Fig. 3G). Both the mRNA

and the fusion protein show elevation in the AER at E9.5 (Fig. 3H). Expression of Atr2 in the AER is required for normal development, as the AER does not form properly in mutant embryos (Fig. 3I,J). E11.5 embryos express Atr2 in a pattern similar to that seen at E10.5, showing an even greater upregulated expression in neurons throughout the neural tube (Fig. 3L,M). We have not analyzed functions of Atr2 in the AER or neurons because mutant embryos die from heart failure shortly after E9.5.

Establishment of the ventral forebrain requires Atr2

The anterior neural region of *om* embryos is morphologically abnormal by E8.5-E9.0 (Fig. 4), indicating that Atr2 is important for normal development of the anterior neural plate. An analysis of a variety of genes by whole-mount in situ hybridization revealed that *om* embryos have an inappropriately patterned neurectoderm at E8.5-E9.0. Nkx2.1 is essential for development of the basal forebrain or hypothalamus in mice (Kimura et al., 1996). At E9.0, *Nkx2.1* is expressed in ventral regions of the telencephalic and diencephalic primordia (Fig. 4A). In *om* mutant littermates, *Nkx2.1* is severely reduced, indicating a reduction of ventral fates (Fig. 4B). *Nkx2.1* is ordinarily induced by prechordal Shh-expressing tissue early in day 8 of development (Shimamura and Rubenstein, 1997). Reduced *Nkx2.1* in *om* could be due either to a failure to induce ventral fates during day 8, or to a failure to maintain these fates after they are established.

To address this question, we looked at two markers of the dorsal forebrain, *Pax6* and *Emx2*, which are required for development of the dorsal forebrain or cerebral cortex (Muzio et al., 2002; Schmahl et al., 1993; Stoykova et al., 1996). At E8.5, *Pax6* and *Emx2* are normally expressed in dorsolateral subregions of the neural plate, excluded from the anteromedial area that is fated to become ventral forebrain (Fig. 4C,E) (Rubenstein et al., 1998). In *om* mutants, both *Pax6* and *Emx2* are abnormally expanded across the anterior midline, indicating an expansion of dorsal fates at the expense of ventral ones (Fig. 4D,F). These data suggest that ventral fates are not induced in *om* embryos.

The anterior midline is defective in *om* embryos

The expansion of *Pax6* and *Emx2* into the anterior neural midline, and the reduction of *Nkx2.1* ventrally, suggested a loss of ventralizing signals. To discover whether such signals were present in *om* embryos, we examined *Shh* expression. Shh is a ventralizing signal produced by the prechordal plate, notochord and prospective floorplate during day 8 (Epstein et al., 1999). Interestingly, in *om* embryos at E8.75, *Shh* expression was normal posterior to the hindbrain, but was almost completely absent from its anterior domain (Fig. 4G; *om* left, wild type right). Only a small spot of *Shh* expression remained in *om* (arrowhead), which was likely responsible for inducing the residual *Nkx2.1* expression (Fig. 4B), and possibly for keeping the central neural plate clear of dorsal-specific transcripts. To determine whether the anterior-specific loss of *Shh* at E8.75 is due to a failure to initiate or a failure to maintain expression, *Shh* expression was examined in very early headfold embryos. In mutants at E8.0, *Shh* is missing from the anteriormost portion of the midline, but is expressed normally in the posterior midline (Fig. 4I). Because the onset of *Shh* expression is very close to E8.0, the lack of transcripts observed at this stage strongly suggests that *Shh* fails to initiate expression in its anterior domain in *om* mutants.

We looked further, for the expression of genes regulated by Shh – *Gli1* and *Gli3* (Ruiz i Altaba, 1998). At E8.75 the normal *Gli1* expression pattern is similar to that of *Shh*, but is wider ventrally (Fig. 4J; wild type right), whereas *Gli3* exhibits a complementary dorsal-restricted pattern (Fig. 4K). *Gli1* was significantly reduced anteriorly in *om* mutants (Fig. 4J; left), whereas *Gli3* was expanded towards the ventral midline (Fig. 4L), consistent with reduced Shh function. *Gli3* encroached on the midline from the forebrain through the posterior hindbrain. These mutant expression patterns illustrate that Atr2 is required for Shh production by midline cells that underlie the developing brain. However, by E9.5, *om* mutants appear to recover normal patterns of *Shh*, *Gli1* and *Gli3* expression (not shown), indicating that the onset of anterior *Shh* expression is significantly delayed in *om* mutants, rather than abolished. We could not explore the effects of this delay on subsequent brain development in any detail because by E9.5, mutants are unhealthy owing to imminent cardiac failure.

Even though no *Shh* deficit was detected in the posterior of mutants during day 8, mutants exhibit incomplete floorplate formation in the spinal cord at E9.5. At E9.5 in normal embryos, *Shh* is expressed in the notochord and neural floorplate; furthermore, the ventral spinal cord midline is thin relative to the lateral edge, reflecting floorplate development (Fig. 4M). In *om* mutants of the same stage, although *Shh* expression is normal, the ventral midline of the spinal cord is not thin, and the notochord is abnormally large (Fig. 4N). Embryos were also stained for *Hnf3b* (*Foxa2* – Mouse Genome Informatics), a floorplate marker and transcription factor involved in inducing *Shh* through direct binding to *Shh* promoter elements (Epstein et al., 1999). At E9.5, mutants express *Hnf3b* normally in the ventral spinal cord, but they show morphological floorplate and notochord abnormalities (Fig. 4P). These results indicate that Atr2 is not required for the expression of floorplate-specific genes in the spinal cord, but that it is necessary for the development of floorplate morphology, and for normal convergence/extension of the notochord.

To determine whether the anterior decrease in *Shh* during day 8 reflected a loss of anterior cells or a specific failure of these cells to express *Shh*, younger mutants were stained for *Hnf3b* and for brachyury (Wilkinson et al., 1990), both markers of the developing notochord. Mutant embryos show normal and robust expression patterns of both *Hnf3b* at E8.5 (Fig. 4R), and brachyury at E8.25 (Fig. 4T). E8.5 embryos were also stained for goosecoid (*gsc*), a marker of the prechordal plate and anterior ventral neural plate (Blum et al., 1992). No difference in *gsc* expression was detected between wild type (Fig. 4U) and mutants (Fig. 4V). These results strongly suggest that anterior midline cells are indeed present in *om* mutants, but that they lack the ability to express *Shh*.

Fgf8 expression is abnormal in the anterior neural ridge (ANR) of *om* embryos

The anterior neural ridge (ANR) is a signaling center involved in patterning the vertebrate telencephalon (Rubenstein et al., 1998; Shimamura and Rubenstein, 1997). The patterning function of the ANR is meditated at least in part by Fgf8, a

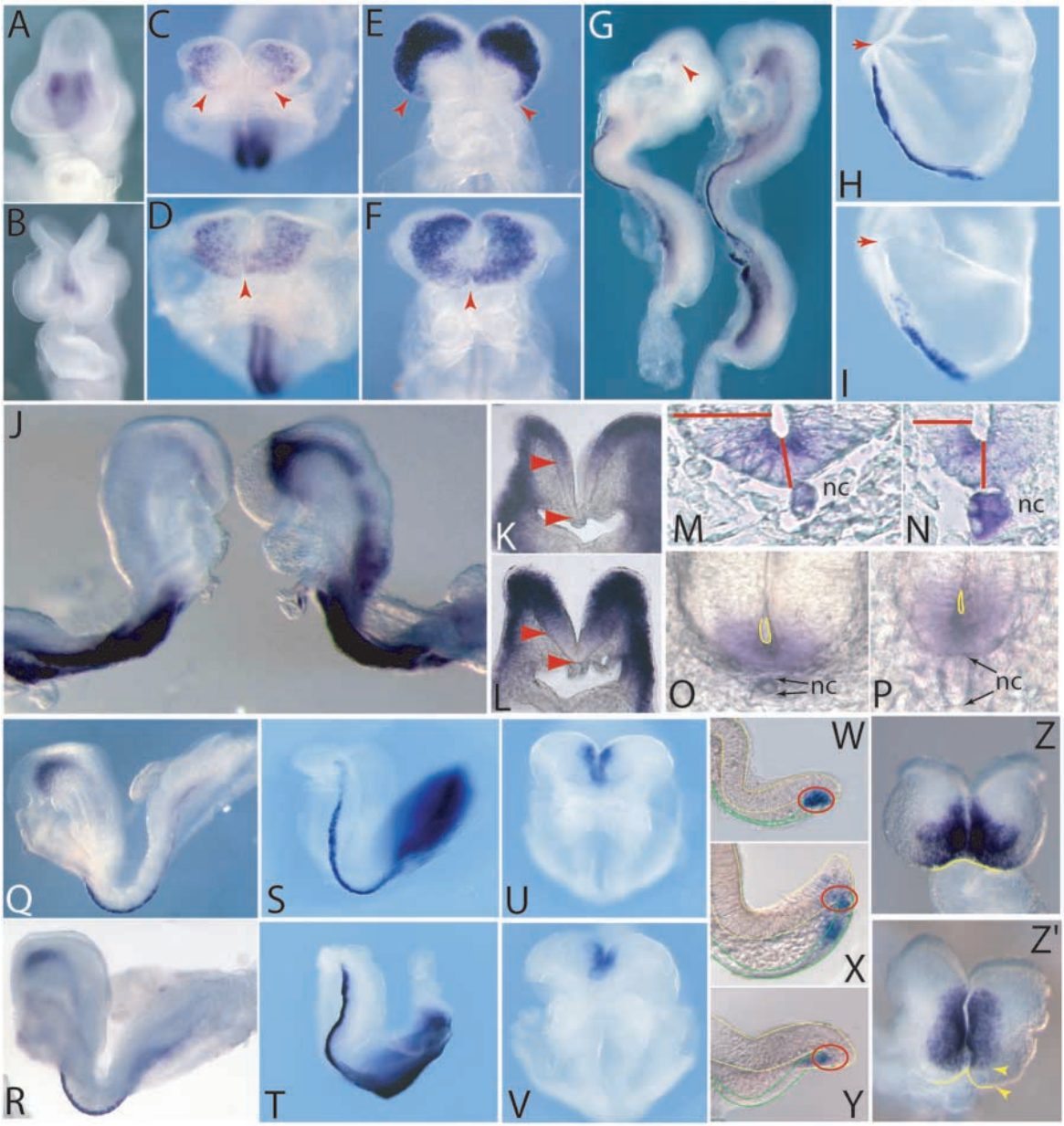

Fig. 4. Atr2 is required for patterning the ventral forebrain and for expression of patterning signals by the anterior notochord and the ANR during E8. (A) A normal E9.5 embryo expresses *Nkx2.1* in the ventral forebrain. (B) An *om* mutant littermate shows reduced *Nkx2.1* expression. (C) At E8.5, *Pax6* is excluded from the anterior neural plate (red arrowheads). (D) In *om* mutants, *Pax6* is abnormally expanded across the anterior midline (red arrowhead). (E) At E8.5, *Emx2* is excluded from the anterior midline (arrowheads). (F) *om* mutants express *Emx2* across the anterior neural midline (arrowhead). (G) At E8.75, *Shh* is diminished in the anterior region of *om* mutants (left) compared with in normal littermates (right), except for a small spot (arrowhead). (H) At E8.0, *Shh* is expressed in the full extent of the developing midline, nearly reaching the anteriormost edge of the neural plate (red arrow). (I) In E8.0 mutants, *Shh* expression is reduced anteriorly. The anterior edge of the neural plate is indicated (red arrow). (J) *Gli1* is reduced in the anterior region of the *om* mutant (left) compared with wild type (right). (K) *Gli3* is normally absent from the midline of the neural plate at E8.75 (arrowheads), as seen in this transverse slice through the hindbrain. (L) In *om*, *Gli3* is expanded toward the midline (arrowheads). (M) At E9.5, transverse sections show *Shh* in the spinal cord floorplate and the notochord (nc) of a wild-type embryo. The floorplate is thinner than the lateral wall (compare red lines). (N) In *om* mutants at E9.5, *Shh* is expressed normally but the notochord is enlarged and the floorplate has not thinned (red lines). (O,P) At E9.5, *Hnf3b* is expressed in the ventral spinal cord in both normal (O) and mutant (P) embryos; mutants have enlarged notochords and an absence of floorplate. Ventral neurocoels are outlined in yellow. (Q) *Hnf3b* expression in a wild-type embryo at E8.5. (R) *Hnf3b* is expressed normally in *om* embryos. (S) Brachyury marks the developing notochord at E8.25. (T) *om* mutants express brachyury normally at E8.25. (U) At E8.5, goosecoid is expressed in the anterior midline. (V) *om* mutants express goosecoid in a wild-type pattern. (W-Y) Parasagittal sections of the anterior neural plate of E8.5 embryos stained with *Fgf8.* Dorsal is up, anterior is right. Epidermal ectoderm is outlined in green, neural tissue in yellow. (W) In wild type, *Fgf8* transcripts are tightly localized to the anterior neural ridge (ANR; red circle). (X,Y) In *om* embryos, *Fgf8* expression is decreased in the ANR (red circles), and is shifted into the adjacent epidermal ectoderm and neurectoderm. (Z) At E8.5, *Hesx1* is expressed in the anterior neural plate up to the ANR (yellow line). (Z′) In *om* embryos, *Hesx1* expression is reduced laterally and is absent from the anteriormost neural plate (yellow arrowheads).

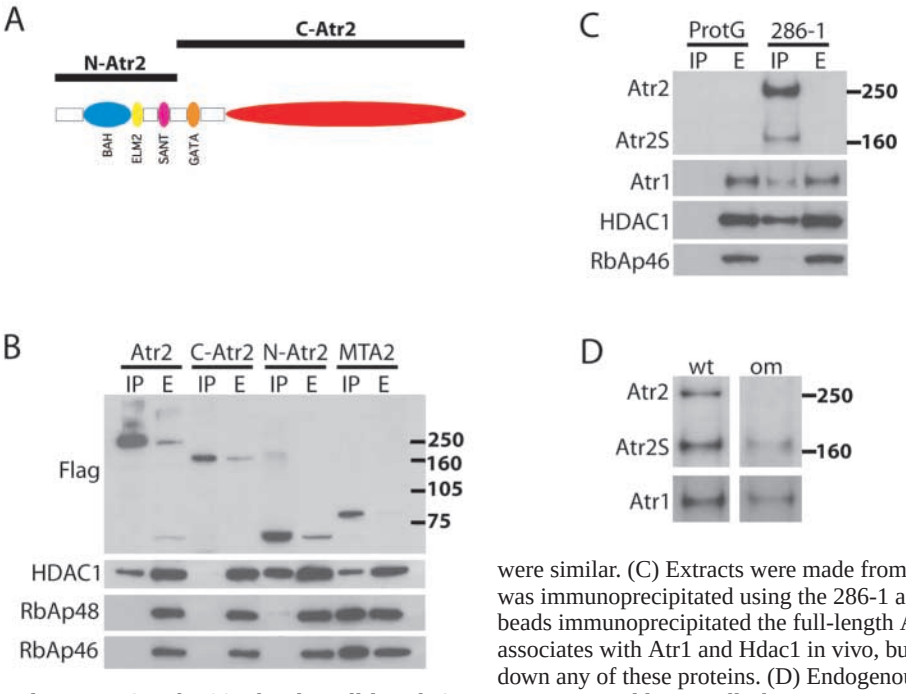

Fig. 5. Atr2 interacts with histone deacetylase 1 in vivo. (A) The domain structure of Atr2 and the fragments used in transfection experiments are illustrated. N-Atr2 encodes the N-terminal BAH, ELM2 and SANT domains. C-Atr2 encodes the rest of the protein, from the GATA domain through the C terminus. (B) Each indicated protein was flag-tagged at the N terminus, overexpressed in 293 cells, then immunoprecipitated using anti-flag beads. Western blots show immunoprecipitated proteins [IP] run next to total soluble extract [E]. Hdac1 is associated with full-length Atr2, N-Atr2 and Mta2, but not with C-Atr2. The NuRD core subunits RbAp48 and RbAp46 are only found in association with Mta2. Extract lanes show that the total protein concentrations in each extract were similar. (C) Extracts were made from wild-type E9.5 embryos, and endogenous Atr2 was immunoprecipitated using the 286-1 antibody linked to protein G sepharose. 286-1 beads immunoprecipitated the full-length Atr2 as well as Atr2S. Endogenous Atr2 associates with Atr1 and Hdac1 in vivo, but not with RbAp46. Protein G beads did not pull down any of these proteins. (D) Endogenous Atr2 was immunoprecipitated from wild-type and *om* MEFS with 286-1 beads. Full-length Atr2 is present in wild-type cells, but is missing in *om* cells; Atr2S was present in both. Atr1 was pulled down with Atr2 in both cell types.

potent signaling molecule required for telencephalic development (Meyers et al., 1998). At E8.5, the ANR is located at the anterior border of the neural plate, at the junction of the ectoderm and neurectoderm. *Fgf8* expression is normally tightly localized within the ANR at this stage (Fig. 4W; red circle) (Crossley and Martin, 1995).

To determine whether ANR signals are produced in *om* mutants, the expression of *Fgf8* was examined. Expression of *Fgf8* in the vicinity of the ANR in mutant embryos is reduced in intensity and delocalized relative to wild type (Fig. 4X,Y). In mutants, *Fgf8* expression is no longer limited to the border between the neurectoderm and the epidermal ectoderm, but spreads abnormally into the epidermal ectoderm and the neuroepithelium. The delocalization of *Fgf8* in mutant embryos indicates that Atr2 is necessary to limit *Fgf8* to the ANR. As Fgf8 can repress *Emx2* (Crossley et al., 2001), reduced Fgf8 signaling may contribute to the expansion of *Emx2* expression observed in the *om* mutant neural plate (Fig. 4F). Hesx1 is a transcription factor required for telencephalic development, and for normal levels of *Fgf8* expression in the ANR (Martinez-Barbera and Beddington, 2001). In *om* embryos, *Hesx1* is maintained in the medial neural plate, but is absent from the ANR and the anterolateral neural plate (Fig. 4Z′). Reduction of *Hesx1* in the mutant ANR may contribute to the observed decrease in *Fgf8* expression.

Atr2 associates with Hdac1 but not other NuRD components

The *Drosophila* genome encodes a single atrophin-related protein (Atro) that functions as a co-repressor for *eve*, and, given the complexity of patterning defects in mutant embryos, probably for other transcription factors as well (Erkner et al., 2002; Zhang et al., 2002). Although the molecular co-repression mechanism for Atro and Eve has not been elucidated, Atro and Atr2 (but not Atr1) show significant N-terminal protein homology to vertebrate metastasis associated factor 2 (Mta2) (Fig. 2A), suggesting they may have a similar function. Mta2 is a core subunit of NuRD, a histone deacetylase complex with transcriptional repressive activity (Zhang et al., 1999). Other NuRD core subunits include Mbd3b, Hdac1, Hdac2, RbAp46, and RbAp48.

To determine whether Atr2 associates with NuRD components in vivo, flag-tagged Mta2 (a gift of D. Reinberg) and full-length flag-tagged Atr2 (Fig. 5A) were transiently overexpressed individually in 293 cells. Soluble extracts were incubated with anti-flag beads to immunoprecipitate transfected and associated proteins. Immunoprecipitated proteins were examined by western blotting for the presence of the transfected protein, and then for NuRD complex proteins using antibodies specific for Hdac1, RbAp48 and RbAp46 (Fig. 5B). Flag-Mta2 yielded the expected band at about 80 kDa, and pulled down Hdac1, RbAp46 and RbAp48, as previously demonstrated (Zhang et al., 1999). Flag-Atr2 migrated at 250 kDa and pulled down Hdac1, but not RbAp46 or RbAp48 (Fig. 5B).

To determine whether the association of Atr2 with Hdac1 was mediated by its Mta2-homologous domains or by another region, the protein was divided into two fragments (Fig. 5A). The N-terminal fragment (N-Atr2) encodes the BAH, ELM2 and SANT domains and the C-terminal fragment (C-Atr2) contains the remainder of the protein, from the GATA domain through the Atr1-homologous region. These fragments were flag-tagged and examined in 293 cells, as described above. These experiments show that Hdac1 immunoprecipitates with N-Atr2, but not with C-Atr2 (Fig. 5B), indicating that sequences through the SANT domain are sufficient for Hdac1 recruitment.

In order to look at the binding partners of Atr2 in mouse

embryos, a polyclonal antibody recognizing the C terminus of Atr2 was produced, called 286-1. This antibody was crosslinked to protein G sepharose beads and used to immunoprecipitate endogenous Atr2 from wild-type E9.5 embryo extracts (Fig. 5C). 286-1 beads pulled down both full-length Atr2, and the ~160 kDa short form of Atr2, Atr2S. Endogenous Atr2 was specifically associated with Atr1 and Hdac1, but not with RbAp46. Thus, Atr2 associates with Hdac1 in 293 cells and in the mouse embryo, but not with the core NuRD subunit RbAp46, suggesting that it exists in a complex distinct from NuRD.

286-1 beads were also used to determine whether any full-length Atr2 is made by *om* cells. Because it was difficult to isolate E9.5 *om* mutants that were both healthy and similar in size to their unaffected littermates, fibroblasts were isolated from E8.75 wild-type and *om* mutant embryos, and grown in culture. Extracts were made from these mouse embryo fibroblasts (MEFs) and endogenous Atr2 immunoprecipitated. Although Atr2S was present in *om* MEFs, no full-length Atr2S could be detected (Fig. 5D). Atr1 was co-immunoprecipitated in wild-type and mutant cells (Fig. 5D), but no robust association with Hdac1 could be found in either cell line (not shown).

Discussion

Signaling centers play an important role in development by inducing and patterning the outgrowth of embryonic structures. Atr2 has an important role in the activity of two signaling centers, the anterior midline and the ANR, and is also likely to function in an organizing center of the limb bud, the AER.

Atr2 is required for *Shh* expression in the anterior midline during day 8 of development

Regulation of the *Shh* expression pattern during mouse development is complex. Multiple enhancers have been discovered, in the both mouse and zebrafish *Shh* promoters, that are responsible for directing *Shh* expression to distinct subdomains of its overall pattern (Epstein et al., 1999; Muller et al., 1999). Along similar lines, we have found that Atr2 is required for *Shh* to be expressed in its anterior subdomain. Atr2 is necessary for initiation of *Shh* in the anterior midline at E8.0, but not in the posterior midline (Fig. 4I). Interestingly, the same anterior midline cells that lose *Shh* in E8.0 mutants, normally upregulate Atr2 at E8.0-E8.25 (Fig. 2A,B), consistent with the idea that a high level of Atr2 is required for *Shh* to be transcribed anteriorly. One of the transcriptional activators of *Shh* is Hnf3β (Ang and Rossant, 1994; Weinstein et al., 1994). *Hnf3b* is expressed in *om* mutants at E8.5 (Fig. 4R), but it is not sufficient to activate *Shh* in the anterior midline. Anterior midline cells are clearly present in *om* mutants, being marked by expression of *Hnf3b*, *gsc*, and brachyury (Fig. 4Q-V). Taken together, these data demonstrate that even though anterior midline cells are present and express a known inducer of *Shh*, they fail to activate *Shh* expression.

This in turn suggests that an Atr2-regulated repressor of *Shh* is expressed in the anterior midline. An apparent candidate for this repressor is *Gli3*, because it is capable of downregulating *Shh* (Ruiz i Altaba, 1998) and is expanded in *om*. However, it is unlikely that the hypothetical Atr2-regulated repressor is Gli3 for the following reasons. First, *Gli3* is still excluded from the ventral-most midline of the brain in *om* mutants (Fig. 4L), where Atr2 is elevated (Fig. 3d). Second, if depression of Gli3 were a direct event in *om* mutants, reducing the dosage of Gli3 by creating compound mutants between *om* and *Gli3 extra-toes* (Hui and Joyner, 1993) should, at least to some extent, rescue ventral development. Instead, double mutants exhibit a more severe phenotype (J.S.Z. and A.S.P., unpublished). Therefore it is more likely that Atr2 silences an as yet unidentified repressor of *Shh* during day 8. Because *om* mutants appear to recover a normal *Shh* expression pattern by E9.5 (not shown), the window of activity of this repressor or the competence to respond to it appears to be limited to day 8 of development. Alternatively, Atr2 may act as an activator of *Shh*.

Atr2 is required to localize Fgf8 to the ANR

Atr2 is also necessary for correct restriction of *Fgf8* to the ANR signaling center, because *om* mutants show reduced and disorganized Fgf8 expression at and around the anterior neural margin (Fig. 4X,Y). Fgf8 signals from the ANR normally contribute to patterning the telencephalic primordia (Eagleson and Dempewolf, 2002; Martinez-Barbera and Beddington, 2001; Rubenstein et al., 1998; Shanmugalingam et al., 2000; Shimamura and Rubenstein, 1997). The mechanisms that ordinarily restrict Fgf8 to the border between the neurectoderm and the epidermal ectoderm are not known. For the midbrain-hindbrain isthmic organizer, another signaling center using Fgf8, *Fgf8* restriction involves complex positive and negative regulatory mechanisms; at the boundary between the Otx2 and Gbx2 expression domains, for example, Otx2 represses *Fgf8* while Gbx2 maintains *Fgf8* expression (Wurst and Bally-Cuif, 2001). By analogy, positioning of *Fgf8* at the ANR is also likely to involve positive and negative influences. In this context, Atr2 appears to act as a requisite component of a transcriptional repressor that is needed both for full-level expression of *Fgf8* from the ANR, and for limiting *Fgf8* expression to the ANR. Hesx1 is a transcriptional regulator that functions in the anterior neurectoderm (Martinez-Barbera et al., 2000). Hesx1 is necessary for full expression of *Fgf8* from the ANR-derived commissural plate (Martinez-Barbera and Beddington, 2001). Atr2 in turn is necessary for the expression of *Hesx1* in the ANR at E8.5 (Fig. 4Z′). Thus a normal role of Atr2 may be to silence a repressor of *Hesx1* in the ANR so that this factor is available to support normal *Fgf8* expression levels. However, this same mechanism of Fgf8 regulation can clearly not be operating in the presumptive telencephalic neurectoderm or the adjacent epidermal ectoderm. We hypothesize the existence of additional repressors, both in the neurectoderm and in the epidermal ectoderm, that cooperate with Atr2 to silence *Fgf8* in these tissues. Although there is a mild upregulation of Atr2 in the isthmus at E9.5 (Fig. 3E), *om* mutants show correct restriction of *Fgf8* transcripts to the isthmus at E9.0 (not shown).

Atr2 is required for normal AER formation

The AER is a specialization of the ectoderm that lies at the dorsoventral boundary of the developing limb bud and that is involved in controlling limb pattern (Capdevila and Izpisua Belmonte, 2001). Atr2 is expressed at high levels in the AER at E9.5 (Fig. 3H-J). When Atr2 function is reduced, AER precursors aggregate abnormally in the center of the limb bud instead of lining up along the boundary (Fig. 3J). Although

death of mutants prior to limb bud outgrowth prevented studying mutant limb phenotypes, Atr2 appears to be required for the correct initial setup of this limb bud organizer. The generation of conditional alleles of Atr2 will allow us to examine the effects of loss of Atr2 on limb patterning.

Does Atr2 play a role in neural degeneration in DRPLA?

Atr2 is strongly expressed in developing neurons (Fig. 3K-M), suggesting it may interact with Atr1 in regulating neuronal development and/or function. A growing body of data points towards dysregulation of transcription as an important pathogenic mechanism in polyglutamine diseases (Freiman and Tjian, 2002). Polyglutamine-expanded proteins can sequester transcriptional regulators like CBP and thereby disrupt transcriptional control (Nucifora et al., 2001). Atr1 and Atr2 bind directly to each other, and their binding is stimulated by expanded glutamine in Atr1 (Yanagisawa et al., 2000), suggesting that the neural degeneration in DRPLA involves depletion of Atr2 and derepression of Atr2 target genes. Dissecting the role of Atr2 in neurons, alone and in conjunction with Atr1, is likely to provide insight into the normal cellular functions of these proteins, and by extension help clarify the molecular mechanisms of neurodegeneration in DRPLA. The study of the neuronal functions of Atr2 will require construction of conditional alleles to allow survival of mutant animals beyond E9.5, which is currently in process.

Atr2 may function as a co-repressor

Although mammalian genomes contain two atrophin genes, the *Drosophila* and *C. elegans* genomes contains only one each, *Atro* and *egl-27*, respectively (Ch'ng and Kenyon, 1999; Erkner et al., 2002; Herman et al., 1999; Solari and Ahringer, 2000; Solari et al., 1999; Zhang et al., 2002). Atro functions during early development as a co-repressor for the Eve transcription factor (Zhang et al., 2002), and later regulates transcription in the planar polarity pathway (Fanto et al., 2003). The widespread expression pattern of *Atro*, and the diverse developmental defects in *Atro* and *egl-27* mutants, strongly suggest that other sequence specific transcription factors also use atrophins as co-repressors. Interaction between Atro and Eve occurs through the C-terminal domain of Atro. An analogous interaction in mammals has also been detected; yeast two-hybrid screens with a mammalian transcriptional repressor have pulled the C-terminal portion of both Atr1 and Atr2 from libraries (V. J. Bardwell and M. W. Murphy, personal communication). Presumably then, the co-repressor function of atrophins is conserved in vertebrates.

Further supporting the co-repressor hypothesis, is the conservation of N-terminal sequences between Atro, EGL-27, Atr2 and Mta2. We have shown that the N-terminal, Mta2-homologous region of Atr2, excluding the GATA domain, is required and sufficient for recruitment of Hdac1 in 293 cells (Fig. 5B). We have also shown that endogenous Atr2 recruits Hdac1 in the mouse embryo (Fig. 5C). Association of Atr2 with a histone deacetylase in vivo is significant, because such proteins alter the structure of chromatin and silence transcription (Ng and Bird, 2000), supporting the idea that Atr2 functions as a transcriptional repressor during development. The fact that Atr2 associates with Hdac1 but not with RbAp46 or RbAp48 suggests that Atr2 acts in a protein context distinct from NuRD. Combining all the available data, we hypothesize that the mechanism of gene silencing by Atr2 involves binding directly to sequence-specific transcription factors, which brings associated histone deacetylases to bear on specific promoters.

We have also observed an association between endogenous Atr2 and Atr1 in mouse embryos and MEFs, providing evidence that these two proteins form heterodimers during embryonic development. As full-length Atr2 was absent from *om* MEFs but an association with Atr1 was still observed, it is clear that Atr2S is able to associate with Atr1. It is unclear why an association between Atr2 and Hdac1 was not seen in MEFs. One possibility is that Atr1 blocks the ability of Atr2 to associate with Hdac1. Additional binding studies are necessary to determine whether Atr2, Atr2S, Atr1 and Hdac1 all exist in a complex together, or if some components are mutually exclusive.

In summary, we have analyzed the phenotype of mutant alleles of *Atr2*, and we have found that Atr2 is required for normal embryonic patterning and for the specific regulation of *Shh* in its anterior domain. We have shown that Atr2 is required for establishment of proper dorsoventral pattern in the anterior neural plate. We have provided evidence that mutant anterior neural pattern results from the disruption of two signaling centers, the anterior midline and the ANR. Finally, in accord with a proposed role for atrophin family members as transcriptional co-repressors, we have presented biochemical evidence that Atr2 can recruit histone deacetylase in vivo. Taken together, these data suggest that the embryonic defects observed in *Atr2* mutants are caused by the loss of a novel histone deacetylase complex and the subsequent derepression of developmentally important genes.

We thank Bill Skarnes and Perry Tate for gene-trap mice and advice; Vivian Bardwell and Steve Kerridge for discussions and communication of results before publication; Danny Reinberg for advice and the gift of the Mta2 expression plasmid; Ray White for a critical reading of the manuscript; Michael Depew for the *gsc* expression construct; Francesca Mariani for the brachyury expression construct; and members of the Peterson laboratory for suggestions and discussions. This work was supported in part by grants from the NIH and the Human Frontiers Science Program to A.S.P. J.S.Z. was supported in part by an individual NRSA. The authors have no competing financial interests. Requests for materials should be directed to A.S.P.

References

Ang, S. L. and Rossant, J. (1994). HNF-3 beta is essential for node and notochord formation in mouse development. *Cell* **78**, 561-574.

Beddington, R. S. and Robertson, E. J. (1998). Anterior patterning in mouse. *Trends Genet.* **14**, 277-284.

Beddington, R. S. and Robertson, E. J. (1999). Axis development and early asymmetry in mammals. *Cell* **96**, 195-209.

Blum, M., Gaunt, S. J., Cho, K. W., Steinbeisser, H., Blumberg, B., Bittner, D. and De Robertis, E. M. (1992). Gastrulation in the mouse: the role of the homeobox gene goosecoid. *Cell* **69**, 1097-1106.

Briscoe, J., Sussel, L., Serup, P., Hartigan-O'Connor, D., Jessell, T. M., Rubenstein, J. L. and Ericson, J. (1999). Homeobox gene Nkx2.2 and specification of neuronal identity by graded Sonic hedgehog signalling. *Nature* **398**, 622-627.

Camus, A., Davidson, B. P., Billiards, S., Khoo, P., Rivera-Perez, J. A., Wakamiya, M., Behringer, R. R. and Tam, P. P. (2000). The morphogenetic role of midline mesendoderm and ectoderm in the development of the forebrain and the midbrain of the mouse embryo. *Development* **127**, 1799-1813.

Capdevila, J. and Izpisua Belmonte, J. C. (2001). Patterning mechanisms controlling vertebrate limb development. *Annu. Rev. Cell Dev. Biol.* **17**, 87-132.

Ch'ng, Q. and Kenyon, C. (1999). *egl-27* generates anteroposterior patterns of cell fusion in *C. elegans* by regulating Hox gene expression and Hox protein function. *Development* **126**, 3303-3312.

Chiang, C., Litingtung, Y., Lee, E., Young, K. E., Corden, J. L., Westphal, H. and Beachy, P. A. (1996). Cyclopia and defective axial patterning in mice lacking Sonic hedgehog gene function. *Nature* **383**, 407-413.

Crossley, P. H. and Martin, G. R. (1995). The mouse Fgf8 gene encodes a family of polypeptides and is expressed in regions that direct outgrowth and patterning in the developing embryo. *Development* **121**, 439-451.

Crossley, P. H., Martinez, S., Ohkubo, Y. and Rubenstein, J. L. (2001). Coordinate expression of Fgf8, Otx2, Bmp4, and Shh in the rostral prosencephalon during development of the telencephalic and optic vesicles. *Neuroscience* **108**, 183-206.

Eagleson, G. W. and Dempewolf, R. D. (2002). The role of the anterior neural ridge and Fgf-8 in early forebrain patterning and regionalization in Xenopus laevis. *Comp. Biochem. Physiol. B Biochem. Mol. Biol.* **132**, 179-189.

Echelard, Y., Epstein, D. J., St-Jacques, B., Shen, L., Mohler, J., McMahon, J. A. and McMahon, A. P. (1993). Sonic hedgehog, a member of a family of putative signaling molecules, is implicated in the regulation of CNS polarity. *Cell* **75**, 1417-1430.

Epstein, D. J., McMahon, A. P. and Joyner, A. L. (1999). Regionalization of Sonic hedgehog transcription along the anteroposterior axis of the mouse central nervous system is regulated by Hnf3-dependent and -independent mechanisms. *Development* **126**, 281-292.

Ericson, J., Muhr, J., Jessell, T. M. and Edlund, T. (1995). Sonic hedgehog: a common signal for ventral patterning along the rostrocaudal axis of the neural tube. *Int. J. Dev. Biol.* **39**, 809-816.

Erkner, A., Roure, A., Charroux, B., Delaage, M., Holway, N., Core, N., Vola, C., Angelats, C., Pages, F., Fasano, L. et al. (2002). Grunge, related to human Atrophin-like proteins, has multiple functions in *Drosophila* development. *Development* **129**, 1119-1129.

Fanto, M., Clayton, L., Meredith, J., Hardiman, K., Charroux, B., Kerridge, S. and McNeill, H. (2003). The tumor-suppressor and cell adhesion molecule Fat controls planar polarity via physical interactions with Atrophin, a transcriptional co-repressor. *Development* **130**, 763-774.

Freiman, R. N. and Tjian, R. (2002). Neurodegeneration. A glutamine-rich trail leads to transcription factors. *Science* **296**, 2149-2150.

Gerhart, J. (2001). Evolution of the organizer and the chordate body plan. *Int. J. Dev. Biol.* **45**, 133-153.

Gunhaga, L., Jessell, T. M. and Edlund, T. (2000). Sonic hedgehog signaling at gastrula stages specifies ventral telencephalic cells in the chick embryo. *Development* **127**, 3283-3293.

Harland, R. and Gerhart, J. (1997). Formation and function of Spemann's organizer. *Annu. Rev. Cell Dev. Biol.* **13**, 611-667.

Hemmati-Brivanlou, A., Stewart, R. M. and Harland, R. M. (1990). Region-specific neural induction of an engrailed protein by anterior notochord in Xenopus. *Science* **250**, 800-802.

Hentges, K., Thompson, K. and Peterson, A. (1999). The flat-top gene is required for the expansion and regionalization of the telencephalic primordium. *Development* **126**, 1601-1609.

Herman, M. A., Ch'ng, Q., Hettenbach, S. M., Ratliff, T. M., Kenyon, C. and Herman, R. K. (1999). EGL-27 is similar to a metastasis-associated factor and controls cell polarity and cell migration in *C. elegans*. *Development* **126**, 1055-1064.

Hui, C. C. and Joyner, A. L. (1993). A mouse model of greig cephalopolysyndactyly syndrome: the extra-toesJ mutation contains an intragenic deletion of the Gli3 gene. *Nat. Genet.* **3**, 241-246.

Kazanskaya, O., Glinka, A. and Niehrs, C. (2000). The role of *Xenopus* dickkopf1 in prechordal plate specification and neural patterning. *Development* **127**, 4981-4992.

Kimura, S., Hara, Y., Pineau, T., Fernandez-Salguero, P., Fox, C. H., Ward, J. M. and Gonzalez, F. J. (1996). The T/ebp null mouse: thyroid-specific enhancer-binding protein is essential for the organogenesis of the thyroid, lung, ventral forebrain, and pituitary. *Genes Dev.* **10**, 60-69.

Kinder, S. J., Tsang, T. E., Wakamiya, M., Sasaki, H., Behringer, R. R., Nagy, A. and Tam, P. P. (2001). The organizer of the mouse gastrula is composed of a dynamic population of progenitor cells for the axial mesoderm. *Development* **128**, 3623-3634.

Martinez-Barbera, J. P. and Beddington, R. S. (2001). Getting your head around Hex and Hesx1: forebrain formation in mouse. *Int. J. Dev. Biol.* **45**, 327-336.

Martinez-Barbera, J. P., Rodriguez, T. A. and Beddington, R. S. (2000). The homeobox gene Hesx1 is required in the anterior neural ectoderm for normal forebrain formation. *Dev. Biol.* **223**, 422-430.

McCampbell, A., Taye, A. A., Whitty, L., Penney, E., Steffan, J. S. and Fischbeck, K. H. (2001). Histone deacetylase inhibitors reduce polyglutamine toxicity. *Proc. Natl. Acad. Sci. USA* **98**, 15179-15184.

Meyers, E. N., Lewandoski, M. and Martin, G. R. (1998). An Fgf8 mutant allelic series generated by Cre- and Flp-mediated recombination. *Nat. Genet.* **18**, 136-141.

Mukhopadhyay, M., Shtrom, S., Rodriguez-Esteban, C., Chen, L., Tsukui, T., Gomer, L., Dorward, D. W., Glinka, A., Grinberg, A., Huang, S. P. et al. (2001). Dickkopf1 is required for embryonic head induction and limb morphogenesis in the mouse. *Dev. Cell* **1**, 423-434.

Muller, F., Chang, B., Albert, S., Fischer, N., Tora, L. and Strahle, U. (1999). Intronic enhancers control expression of zebrafish sonic hedgehog in floor plate and notochord. *Development* **126**, 2103-2116.

Muzio, L., DiBenedetto, B., Stoykova, A., Boncinelli, E., Gruss, P. and Mallamaci, A. (2002). Conversion of cerebral cortex into basal ganglia in Emx2(–/–) Pax6(Sey/Sey) double-mutant mice. *Nat. Neurosci.* **5**, 737-745.

Ng, H. H. and Bird, A. (2000). Histone deacetylases: silencers for hire. *Trends Biochem. Sci.* **25**, 121-126.

Nucifora, F. C., Jr, Sasaki, M., Peters, M. F., Huang, H., Cooper, J. K., Yamada, M., Takahashi, H., Tsuji, S., Troncoso, J., Dawson, V. L. et al. (2001). Interference by huntingtin and atrophin-1 with cbp-mediated transcription leading to cellular toxicity. *Science* **291**, 2423-2428.

Ross, C. A. (2002). Polyglutamine pathogenesis: emergence of unifying mechanisms for Huntington's disease and related disorders. *Neuron* **35**, 819-822.

Rubenstein, J. L. and Beachy, P. A. (1998). Patterning of the embryonic forebrain. *Curr. Opin. Neurobiol.* **8**, 18-26.

Rubenstein, J. L., Shimamura, K., Martinez, S. and Puelles, L. (1998). Regionalization of the prosencephalic neural plate. *Annu. Rev. Neurosci.* **21**, 445-477.

Ruiz i Altaba, A. (1998). Combinatorial Gli gene function in floor plate and neuronal inductions by Sonic hedgehog. *Development* **125**, 2203-2212.

Saude, L., Woolley, K., Martin, P., Driever, W. and Stemple, D. L. (2000). Axis-inducing activities and cell fates of the zebrafish organizer. *Development* **127**, 3407-3417.

Schmahl, W., Knoedlseder, M., Favor, J. and Davidson, D. (1993). Defects of neuronal migration and the pathogenesis of cortical malformations are associated with Small eye (Sey) in the mouse, a point mutation at the Pax-6-locus. *Acta Neuropathol. (Berl)* **86**, 126-135.

Shanmugalingam, S., Houart, C., Picker, A., Reifers, F., Macdonald, R., Barth, A., Griffin, K., Brand, M. and Wilson, S. W. (2000). Ace/Fgf8 is required for forebrain commissure formation and patterning of the telencephalon. *Development* **127**, 2549-2561.

Shawlot, W., Wakamiya, M., Kwan, K. M., Kania, A., Jessell, T. M. and Behringer, R. R. (1999). Lim1 is required in both primitive streak-derived tissues and visceral endoderm for head formation in the mouse. *Development* **126**, 4925-4932.

Shedlovsky, A., Guenet, J. L., Johnson, L. L. and Dove, W. F. (1986). Induction of recessive lethal mutations in the T/t-H-2 region of the mouse genome by a point mutagen. *Genet. Res.* **47**, 135-142.

Shimamura, K. and Rubenstein, J. L. (1997). Inductive interactions direct early regionalization of the mouse forebrain. *Development* **124**, 2709-2718.

Solari, F. and Ahringer, J. (2000). NURD-complex genes antagonise Ras-induced vulval development in Caenorhabditis elegans. *Curr. Biol.* **10**, 223-226.

Solari, F., Bateman, A. and Ahringer, J. (1999). The *Caenorhabditis elegans* genes *egl-27* and *egr-1* are similar to MTA1, a member of a chromatin regulatory complex, and are redundantly required for embryonic patterning. *Development* **126**, 2483-2494.

Spemann, H. and Mangold, H. (1924). Über induction von Embryonalanlagen durch inplantation Artfremder Organisatore. *Wilhem Roux's Arch. Entw. Mech.* **100**, 599-638.

Stoykova, A., Fritsch, R., Walther, C. and Gruss, P. (1996). Forebrain patterning defects in Small eye mutant mice. *Development* **122**, 3453-3465.

Waerner, T., Gardellin, P., Pfizenmaier, K., Weith, A. and Kraut, N. (2001). Human rere is localized to nuclear promyelocytic leukemia oncogenic domains and enhances apoptosis. *Cell Growth Differ.* **12**, 201-210.

Weinstein, D. C., Ruiz i Altaba, A., Chen, W. S., Hoodless, P., Prezioso, V. R., Jessell, T. M. and Darnell, J. E., Jr (1994). The winged-helix transcription factor HNF-3 beta is required for notochord development in the mouse embryo. *Cell* **78**, 575-588.

Wilkinson, D. G., Bhatt, S. and Herrmann, B. G. (1990). Expression pattern of the mouse T gene and its role in mesoderm formation. *Nature* **343**, 657-659.

Wood, J. D., Nucifora, F. C., Jr, Duan, K., Zhang, C., Wang, J., Kim, Y., Schilling, G., Sacchi, N., Liu, J. M. and Ross, C. A. (2000). Atrophin-1, the dentato-rubral and pallido-luysian atrophy gene product, interacts with ETO/MTG8 in the nuclear matrix and represses. *J. Cell. Biol.* **150**, 939-948.

Wurst, W. and Bally-Cuif, L. (2001). Neural plate patterning: upstream and downstream of the isthmic organizer. *Nat. Rev. Neurosci.* **2**, 99-108.

Yanagisawa, H., Bundo, M., Miyashita, T., Okamura-Oho, Y., Tadokoro, K., Tokunaga, K. and Yamada, M. (2000). Protein binding of a DRPLA family through arginine-glutamic acid dipeptide repeats is enhanced by extended polyglutamine. *Hum. Mol. Genet.* **9**, 1433-1442.

Zhang, S., Xu, L., Lee, J. and Xu, T. (2002). Drosophila atrophin homolog functions as a transcriptional corepressor in multiple developmental processes. *Cell* **108**, 45-56.

Zhang, Y., Ng, H. H., Erdjument-Bromage, H., Tempst, P., Bird, A. and Reinberg, D. (1999). Analysis of the NuRD subunits reveals a histone deacetylase core complex and a connection with DNA methylation. *Genes Dev.* **13**, 1924-1935.

Zoltewicz, J. S. and Gerhart, J. C. (1997). The Spemann organizer of Xenopus is patterned along its anteroposterior axis at the earliest gastrula stage. *Dev. Biol.* **192**, 482-491.

Zoltewicz, J. S., Plummer, N. W., Lin, M. I. and Peterson, A. S. (1999). oto is a homeotic locus with a role in anteroposterior development that is partially redundant with Lim1. *Development* **126**, 5085-5095.